Applied Acoustics 163 (2020) 107239

Contents lists available at ScienceDirect

Applied Acoustics

journal homepage: www.elsevier.com/locate/apacoust

Technical note

Modelling sound absorption properties of broom fibers using artificial neural networks

Gino Iannace *, Giuseppe Ciaburro, Amelia Trematerra

Dipartimento di Architettura e Disegno Industriale, Università degli Studi della Campania Luigi Vanvitelli, 81031 Aversa, Italy

ARTICLE INFO

Article history:
Received 10 December 2019
Received in revised form 23 January 2020
Accepted 29 January 2020

Keywords:
Natural materials
Sound absorption coefficient
Deep neural network
Acoustic measurements

ABSTRACT

The use of broom to produce fibers has ancient roots. The Greeks appreciated its resistance to water and for this reason they used it to manufacture sailing ropes. But broom fiber was also appreciated for its sound absorption qualities. In this study, a new methodology was developed for the numerical modeling of the acoustic behavior of broom fibers. First, the characteristics of the different varieties of broom were examined and the procedures for processing the samples to be analyzed were described. Subsequently, the results of the measurements of the following acoustic properties of the material were analyzed: air flow resistance, porosity, and sound absorption coefficient. Finally, the results of the numerical modeling of the acoustic coefficient were reported using an algorithm based on artificial neural networks. The results obtained are compared with a model based on linear regression. The model based on neural networks showed high values of the Pearson correlation coefficient (0.989), indicating a high number of correct predictions.

1. Introduction

In the construction of a building, the choice of materials represents an important challenge that influences the entire production process. Over the centuries, to reduce energy and environmental costs, as well as to better adapt the building to the climatic conditions of the place, the materials for the construction of the buildings were chosen according to the abundant availability in the construction area. Today this choice is imposed by the need to use natural materials for sustainable and environmentally friendly construction. The high recyclability of natural materials, which can be used in low-cost constructions, combined with simple and traditional construction techniques capable of exploiting the bioclimatic principles for energy needs, allow us to create ecologically aware and responsible constructions, capable of responding to the different needs of the users [1,2].

If in the past the choice of a material derived from the experience of the master builder, today every construction material is first studied to characterize its properties. Some natural materials are characterized by excellent performance properties both from a thermal and acoustic point of view. This is due to the good mechanical properties they possess despite being characterized by low density [3]. Furthermore, they are easy to work with and once prepared they have a high stability. Another feature that distinguishes them is the minimal impact on health and the environment, both in the manufacturing process and in that of use during the entire life cycle [4].

The natural materials of interest from the point of view of acoustic properties are the porous ones: The sound enters the pores and is then dissipated. The large family of natural porous materials includes diversified characteristics that allow us to classify them based on microscopic structures. In this way we can identify three large groups as follows: cellular, fibrous, and granular [5,6].

Natural fibers can be classified according to their origin which can be animal, vegetable or mineral. Animal fibers, such as silk and linen are used mainly in the textile sector. The vegetable fibers are mainly formed by cellulose, hemicellulose and lignin. Their origin is varied in that they come from many plants, even different from each other, and from different plant organs. Pineapple, banana and sisal fibers are extracted from the leaves; from the stem the broom, kenaf, hemp, jute, bamboo; from the fruit the coconut and from the seed the cotton. Finally, there are mineral fibers characterized by a limited length [7].

In the past, several studies have tried to model the acoustic properties of natural fibers. Delany and Bazley [8] have developed a model for absorbent fibrous materials that calculates the

* Corresponding author.
E-mail addresses: gino.iannace@unicampania.it (G. Iannace), giuseppe.ciaburro@unicampania.it (G. Ciaburro), amelia.trematerra@unicampania.it (A. Trematerra).

https://doi.org/10.1016/j.apacoust.2020.107239
0003-682X/

coefficient of sound absorption based on the following parameters: characteristic impedance, angular frequency, sound speed, and flow resistivity. These authors, based on experimental measurements carried out on high porosity fibrous materials, provide simple relationships for the calculation of characteristic quantities. The model assumes that the flow resistivity is enough to determine the characteristic wave impedance and the characteristic propagation constant in the porous material. Subsequently, Miki [9] derived new regression models based on experimental data deriving from the work of Delany and Bazley. The changes concerned the impedance function that now satisfies the positive-real property and the propagation constant written in terms of complex variables that becomes a regular function. In the work of Allard [10] new empirical expressions are elaborated based on the phenomenological equations of Delany and Bazley. The Allard equations work better at low frequencies than those of Delany and Bazley. Based on the general frequency dependence of viscous forces on porous materials, this model suggests that the propagation of sound in fibrous materials depends on both the diameter of the fibers and the density of the material.

A new empirical model was then introduced by Garai et al. [11] which, through reasoning like that followed by Miki, allowed Denaly and Bazley's model to be expanded to include a new class of polyester fiber material. This model is better suited to textile fibers than the coefficients originally proposed by Delany–Bazley. Other authors have developed empirical models for specific fibrous materials (kenaf, juta, fique) by adapting the empirical formulas of Delany and Bazley and developing new coefficients that better approximate the acoustic properties of individual materials [12–15]. Berardi et al. [16] measured absorption coefficient and flow resistance for different natural fibrous materials: Kenaf, wood, hemp, coconut, cork, dog, cardboard, and sheep wool. The authors then applied the existing empirical models for the prediction of the acoustic behavior of these materials. From the comparison with the measured values they highlighted the limits of the theoretical models defined for porous materials with homogeneous fibers, when applied to natural materials. They applied an inverse optimization method to estimate the coefficients that best describe the acoustic impedance and the propagation constant for several natural fibers.

The microscopic structure of natural fibers is characterized by an irregular shape which represents the main limit of theoretical models in predicting the coefficient of sound absorption of these materials. In the present work, a new methodology is elaborated for the numerical modeling of the acoustic behavior of broom fibers. First the characteristics of the different varieties of broom are examined and the procedures for processing the samples to be analyzed are described. Subsequently, the results of the measurements of the following acoustic properties of the material are reported: sound absorption coefficient, air flow resistance and porosity. Finally, the results of the numerical modeling of the acoustic coefficient are reported using an algorithm based on artificial neural networks. The results obtained are compared with a model based on linear regression.

2. Methodology

2.1. Broom fibers characterization

The brooms are perennial woody shrubs with a height ranging from half a meter up to 5 m, belonging to the Fabaceae family. The stem is erect and very branched. The branches are like those of the rush and are green. The leaves are sessile, small, linear in shape and fall very early, so that they are almost completely absent at flowering. Therefore, the green branches replace the leaves in chlorophyll photosynthesis. The flowers are collected in terminal racemes, they are papilionaceous, of an intense yellow color and very fragrant. The fruit is a green pod covered with hair that turns black and hairless when ripe. The seeds are dark brown and are very toxic but appreciated by birds.

The wild variety grows on hills and mountains of the Mediterranean countries. The broom prefers very poor soils and has a long life (Fig. 1).

Two types of brooms have been studied: *Spartium junceum*, and *Cytisus scoparius*. The *Spartium junceum* has a cylindrical, hollow and fibrous stem, with strong green branches characterized by an extreme elasticity. The *Cytisus scoparius* has a striped and angular stem, with green and straight branches, which become dark brown after drying. This plant assumes an industrial importance in the textile sector where the fiber obtained from steam is used to produce ropes and fabrics. In the past it was used for the consolidation of embankments and slopes along the railways and highways thanks to its roots that develop deep into the ground [17,18].

The broom is a legume that also lives in arid climates and bears winter frost. It has ecological virtues, because it fixes the atmospheric nitrogen directly without the need for synthetic fertilizers. The textile fibers, obtained from the youngest branches, called vermene, and worked with procedures similar to those of linen and hemp, were already used by the ancient populations to make ropes, baskets, fishing nets and fabrics for the sails, for his sturdy and salt-resistant fiber. Recently, the fibers obtained from the broom have been used as a substitute for glass fiber in the automotive field and in green building, because it is hardly flammable and reduces the toxicity of the fumes in case of fire. These uses suggest deepening the characteristics of broom fibers [19,20].

In order to study the acoustic characteristics, the branches of the brooms were cut in the summer after losing the leaves. The obtained branches were placed on grids for drying in a well ventilated and warm place for about 6 months. The drying process was monitored to avoid decomposition and mold growth problems. Subsequently the branches of the brooms were cut into pieces 200 mm long on average and were divided according to the fiber diameter. In particular, the pieces of broom were grouped for a diameter of 1.5 mm, 3 mm and 4 mm, as shown in Fig. 2.

The dried broom pieces were subsequently assembled with a random distribution in samples held together by an acoustically transparent mesh.

Fig. 1. A field of brooms in hilly terrain.

Fig. 2. Detail of the pieces of broom branches after drying, grouped by diameter. On the left with a diameter of 1.5 mm, in the center with a diameter of 3 mm, on the right with a diameter of 4 mm.

2.2. Measurements of acoustic features

Three acoustic properties were measured: airflow resistance, porosity, and sound absorption coefficient. The air flow resistance is a measure of the resistance that air encounters when passing through the material. The procedure to be followed for its measurement is described in the international standard ISO 9053: 1991 [21]. The standard provides two methods for determining the resistance to air flow. A first method uses a direct air flow, created by conveying a unidirectional air flow through the material and measuring the pressure difference between the two faces of the sample. A second method uses an alternating air flow, with a frequency of 2 Hz and measuring the effective pressure difference on the two sides of the sample placed inside a measurement chamber [22]. In this study the method with alternating air flow was used. In the Fig. 3 is shown the system used for the measurement of the air flow resistivity.

The device in Fig. 3 consists of a closed cylindrical tube which presents the sample of the tested material at one end. At the other end a piston system, moved by a rotating cam, creates the alternating air flow inside the tube. A pressure microphone placed inside the tube measures the pressure disturbance.

Porosity is defined as the ratio between the volume of the fluid contained in the pores and the total volume occupied by the sample, thus providing the fraction of air volume inside the material. When determining porosity, closed pores must not be included in the total volume of air since they are not involved in the propagation of sound waves within the material. In the literature different methods for the measurement of porosity are described. They difference are based on the medium used to saturate the pores of the material, which can be air or water, usually. Moreover, for the method of calculating the volume of air inside the sample. In this case we used water and the porosity was calculated using the following formula:

$$porosity = 1 - \frac{\rho_m}{\rho_{solid}}$$

Here,

- ρ_m (kg/m^3) is the apparent density of the material
- ρ_{solid} (kg/m^3) is the density of the material

Density is the ratio between mass and volume of the sample. The apparent density is calculated by first weighing the sample and subsequently immersing the sample in a graduated glass tube containing water. By reading how much the water level rises we can derive the total volume of the sample. The density of the solid is calculated by a similar procedure only that this time after weighing it the sample is ground and subsequently immersed in water.

The normal incidence sound absorption coefficient was measured in accordance with ISO 10534-2: 1998 [23,24]. The standard describes the procedure for measuring acoustic parameters through small samples that are easy to assemble: the measurements were performed using a Kundt test tube. This device consists of a 56 cm long tube with an internal diameter of 10 cm. The tube diameter corresponds to a higher frequency limit of 2000 Hz. The dimensions of the Kundt tube and the two ¼″ measurement microphones placed at 5 cm allow an accurate measurement of the sound absorption with a lower frequency limit of 200 Hz (Fig. 4).

As already anticipated, to carry out the measurements of the acoustic parameters with the Kundt tube, the dried broom pieces were assembled with a random distribution in samples held together by an acoustically transparent mesh. Three types of broom pieces were used: 1.5 mm, 3 mm and 4 mm diameter size.

Fig. 3. Measuring equipment used for air flow resistance measurements with the alternating air flow method.

Fig. 4. Tube of Kundt, for the absorption coefficient measurements.

The pieces of broom grouped by diameter were then assembled into specimens with a thickness of 60 mm, 80 mm, and 120 mm.

2.3. Artificial neural network model

Machine learning is a sector of artificial intelligence that gathers a set of methods, developed starting from the last decades of the twentieth century in various scientific communities. Machine learning algorithms have been widely used in various fields of use [25–37]. In this work, we will use an algorithm based on artificial neural networks for predicting the sound absorption coefficient of the broom fibers. Neural networks represent a very powerful set of tools that allows solving problems in the field of classification, regression and non-linear control. In addition to having a high processing speed, neural networks can learn the solution from a certain set of examples. In many applications this allows us to overcome the need to develop a model of the physical processes underlying the problem, which can often be difficult, if not impossible, to find [38].

The fundamental element of a neural network is the artificial neuron. A neuron is a device capable, based on a certain number of input signals, of producing an output signal. The input signals, coming from other neurons, are processed through the so-called activation function. Positive signals are excitatory, negative ones are inhibitory. The activation function operates in this way: a weight is assigned to each of the input signals; therefore, the signals are added together. In some more complex models, the activation function also uses the value of the signal that the neuron presented at the output before the new signals were applied. In this way the neuron is a degree of self-excitement so that, in the presence of excitation signals, the passage from the inactive to the excited state is accelerated, while in the absence of new excitation signals, the passage from the excited state to the state inactive is slowed down. The value obtained by the activation function is then passed to the transfer function, which has the purpose of generating the output signal. In a neural network the individual neurons are organized in layers. There are three types of layers: the entry layer, the exit layer, and the hidden layer. The neurons of the entrance layer receive data from the outside world. The output layer neurons present the result of data processing by the neural network. Fig. 5 shows the architecture of a three-layer artificial neural network [39,40].

The transformation of the input x into the weighted output y takes place according to the following equation

$$y = \sum_i w_i * x_i$$

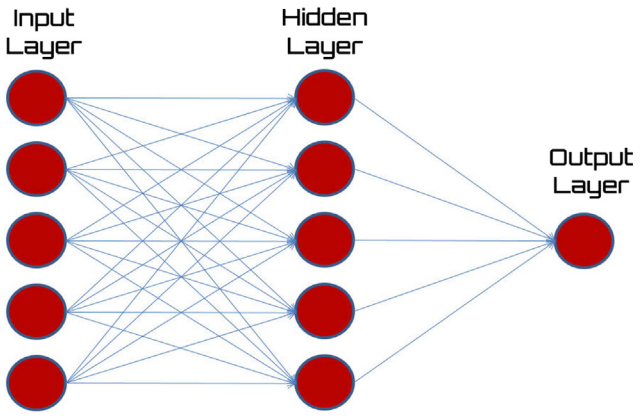

Fig. 5. Architecture of a generic Artificial Neural Network. The nodes and their weighted connections are shown.

Here:

- x_i is the ith input
- w_i is the ith weight
- y is the output

The weights are adjusted based on the experience acquired by the network during the training phase. Training is the process by which we reach the determination of weights and can be a very intense computational action. However, once the weights have been defined, new inputs can be processed very quickly. To train a network we need a set of examples, called a training set, whose elements are input-target pairs. The training consists in searching for the values for the parameters that minimize an appropriate error function [41,42].

The prediction model developed is based on the construction of a multilevel artificial neural network, feed-forward type, with 1 hidden layer (with 10 neurons) and an output that represents the sound absorption coefficient of the material. To estimate the model's generalization capability, the data was divided into two groups, the selection was randomly performed. This selection split the data into two sub-sets:

- 70% of the available observations were used to create a training set. This subset is used by the network during training in which the connection weights are adjusted based on the error made on the output production. This set contains 5720 observations.
- The remaining 30% of the available observations are used to create a test set. This subset has no effect on training and therefore gives us the possibility to check the prediction capability of the network when it receives an input never seen before. This set contains 2452 observations.

In the training phase, the network is used to predict the sound absorption coefficient based on input data. In this phase the data already available are used to compare them with those predicted by the model in order to calculate the forecast error. This error is then used to adjust the weights of the connections. To do this an iterative procedure is followed in order to minimize the error function, with the determination of the weight values made in subsequent steps.

At each step two different phases can be distinguished: In the first phase, the derivatives of the error function with respect to the weights are calculated. In the second phase, the derivatives are used to calculate the new net weights. The Backpropagation algorithm is based on the gradient descent method to find the minimum of the error function with respect to the weights [43]. The gradient descent technique is since the gradient indicates the direction of maximum growth/decrease.

We used a variant of the conjugate gradient methods, the SCG algorithm (Scaled Conjugate Gradient Backpropagation) [44]. SCG returns a super linear convergence in most problems. It provides high performance resulting in at least an order of magnitude faster than the Backpropagation algorithm. Using a step size resizing mechanism, SCG avoids a long search by row for learning iteration, which makes the algorithm faster than other recently proposed second order algorithms.

2.4. Linear regression model

To appreciate the results obtained with the model based on neural networks, we will compare them with those obtained with a model based on multiple linear regression. The regression model serves to establish the relationship between a dependent variable and one or more independent or explanatory variables. In a regression model, the independent variables, called regressors, explain

the dependent variable and allow to understand if there is a trend that allows to make predictions. The dependent variable in the regression equation is modeled as a function of the independent variables plus an error term. The latter is a random variable and represents an uncontrollable and unpredictable variation in the dependent variable. The parameters are estimated in order to better describe the data [45].

Generalized linear models [46] are models that include linear ones and are a natural extension of them. We consider the case in which the response function is not linear, and the variables are not normal. This new class of models is not very wide from a strictly mathematical point of view, but it is flexible enough to incorporate many situations relevant to practical applications. The glm() function of the R software [47] was used to construct the model. The model is set up by providing a symbolic representation of the linear predictor and a description of the error distribution. The distribution of the response as Gaussian and the linking function from the expected value of the distribution to its parameter as identity have been specified.

Several metrics were used to verify the model results. First, we used the root mean square error (RMSE) [48]. The RMSE is the square root of the mean square error, it is the standard deviation of the residual between the values of the observed data and the values of the estimated data. The RMSE varies between zero and $+\infty$ and indicates a deterioration in performance as the value increases. To calculate RMSE, the following equation was used:

$$RMSE = \sqrt{\frac{\sum_{i=1}^{n}(y - y')^2}{n}}$$

Here,

- y is the actual value
- y′ is the predicted value
- n is the number of observations.

The second metric used was the Mean absolute error (MAE). The MAE represents an average of the absolute values of the differences between actual values expected. This is a linear score that fairly balances all individual differences. In fact, it measures the average entity of the errors without considering their direction [48]. To calculate MAE, the following equation was used:

$$MAE = \frac{1}{n} * \sum_{i=1}^{n} |y - y'|$$

Here,

- y is the actual value
- y′ is the predicted value
- n is the number of observations.

Finally, to have a direct measure of the correlation between real values and values predicted by the model, we used the Pearson correlation algorithm [46]. The values of this index vary between −1 and +1, both extreme values represent perfect relations between the variables, while 0 represents the absence of relationship.

2.5. Data preparation

Modeling procedures depend heavily on the quality of input data. Data extracted from various sources and collected in datasets may present anomalies that must be identified and corrected. In our case the dataset contains the results of the measurements so possible attributes or missing records, records without values of certain attributes, values available only in aggregate form, are to be excluded. Since predictors contain very different characteristics, what is needed is data scaling. In fact, the input variables are characterized by different units of measurement which make the ranges of values very different.

A procedure of fundamental importance in statistics and data analysis is the standardization of variables. Through this statistical procedure it is possible to make identical variables belonging to different distributions, but also different variables, or variables expressed in different units of measurement comparable. Standardization is a double normalization. In the first normalization every datum is transformed into its deviation from the mean, in the second normalization this gap is transformed by the unit of measurement or account of that variable in units of its standard deviation.

In this way, each point of the starting distribution corresponds to one and only one point of the new one and retains its relative distances from any other point. Since the original data have been transformed into deviations from the mean, and the algebraic sum of the deviations from the mean is equal to zero, all the standardized variables have an average of zero. Moreover, since each gap from the average is then divided by the standard deviation of the starting variable, the standard deviation of any standardized variable is equal to 1. In this article we used the z score standardization. With this standardization, we subtract the average of the column for each value in a column and then divide the result by the standard deviation of the column. To do this, just apply the following formula:

$$x_{scaled} = \frac{x - mean(x)}{sd(x)}$$

Here,

- mean(x) is the mean of the x
- sd(x) is the standard deviation of the x

As a result, we get features resized to have the properties of a standard normal distribution as follows:

- mean = 0
- standard deviation = 1

Finally, we will have that the values above the mean will be transformed into positive z scores, while the values below the mean will be transformed into negative z scores. The z score is a dimensionless quantity, obtained by subtracting the population average from a single approximate score and then dividing the difference by the population standard deviation [45].

After standardizing the data, it is necessary to proceed with data splitting. Our goal is to develop an algorithm based on neural networks to predict the sound absorption coefficient from some material characteristics. When using a machine learning model, it is necessary to perform model validation. This procedure verifies the model's prediction capability if input data that has never been seen by the network is used. One of the problems that can occur with these models is the excess of adaptation, which means that the model adapts to the observed data because it has an excessive number of parameters with respect to the number of observations. In this case it is necessary to divide the entire data set into two subsets: the training set and the test set. The training set will contain the data that will be used to train the model, while the test set will contain the data that has not been seen so far by the model. The test data set as the data set that the model will probably see in the future. Therefore, the precision we see on the test data set is probably the accuracy of the model on the future data set [42].

In our case, we divided the data into two sets: a training set equal to 70% of the data, and a test set equal to the remaining 30% of the data. The subdivision of the observations in both was carried out randomly.

3. Results and discussion

3.1. Measurements results

As already anticipated, the pieces of broom were grouped corresponding to three types of diameters: 1.5, 3, and 4 mm. For each diameter, the resistivity and porosity were measured according to the methodology already described in the previous section. Table 1 shows the results of the measurements.

Table 1 shows resistivity and porosity values which decrease with increasing diameter. This is since the arrangement of the pieces of broom in the sample becomes increasingly chaotic as the diameter of the pieces increases, thus leaving more pores between the pieces. Furthermore, the random positioning of the pieces gave particularly low values of the air flow resistivity. For the same reason, also the measured porosity was generally low, with a value between 0.76 and 0.65 for increasing diameters.

Table 1
Resistivity and porosity values for each diameter of the broom fibers.

Diameter [mm]	Resistivity [Rayl/m]	Porosity
1.5	762	0.76
3	543	0.67
4	430	0.65

The pieces of broom were subsequently assembled, for each diameter, obtaining three samples with thicknesses of 6 cm, 8 cm and 12 cm respectively. To measure the sound absorption coefficient, the pieces of broom were inserted into the Kundt tube and blocked by an acoustically transparent grid with large meshes. Fig. 6 shows the results of the sound absorption measurements on broom samples of different thickness and with pieces of diameter.

Analyzing the results of the measurement of the acoustic absorption coefficient shown in Fig. 6, it is possible to notice that for each diameter the samples of diameter 60 and 80 mm have returned comparable values. In fact, the curves are similar with only one maximum at a frequency that decreases with increasing sample thickness. Furthermore, the coefficient values move towards lower frequencies for thicker samples. Something different happens for the 120 mm thickness, in this case the curve has two maxima, of which the first occurs at a lower frequency than the lower thicknesses. This behavior is typical of granular materials [49].

Let us now analyze the results obtained for the three types of diameter individually. Samples composed of fragments with a diameter of 1.5 mm generally have values below 0.6. Only the sample with a thickness of 12 cm shows values higher than 0.6, and this happens starting from the frequency of 1500 Hz onwards, with a maximum value around the frequency of 1700 Hz. Samples composed of fragments with a diameter of 3 mm, have slightly higher values than the previous one, however generally the values do not exceed 0.7, if not for the greater thickness (120 mm). This happens both around the first maximum around the 500 Hz frequency and for the second maximum starting from the 1500 Hz frequency. In this case, around the second maximum, the value of the sound absorption coefficient reaches 0.9. Finally, samples composed of fragments with a 3 mm diameter showed significantly lower

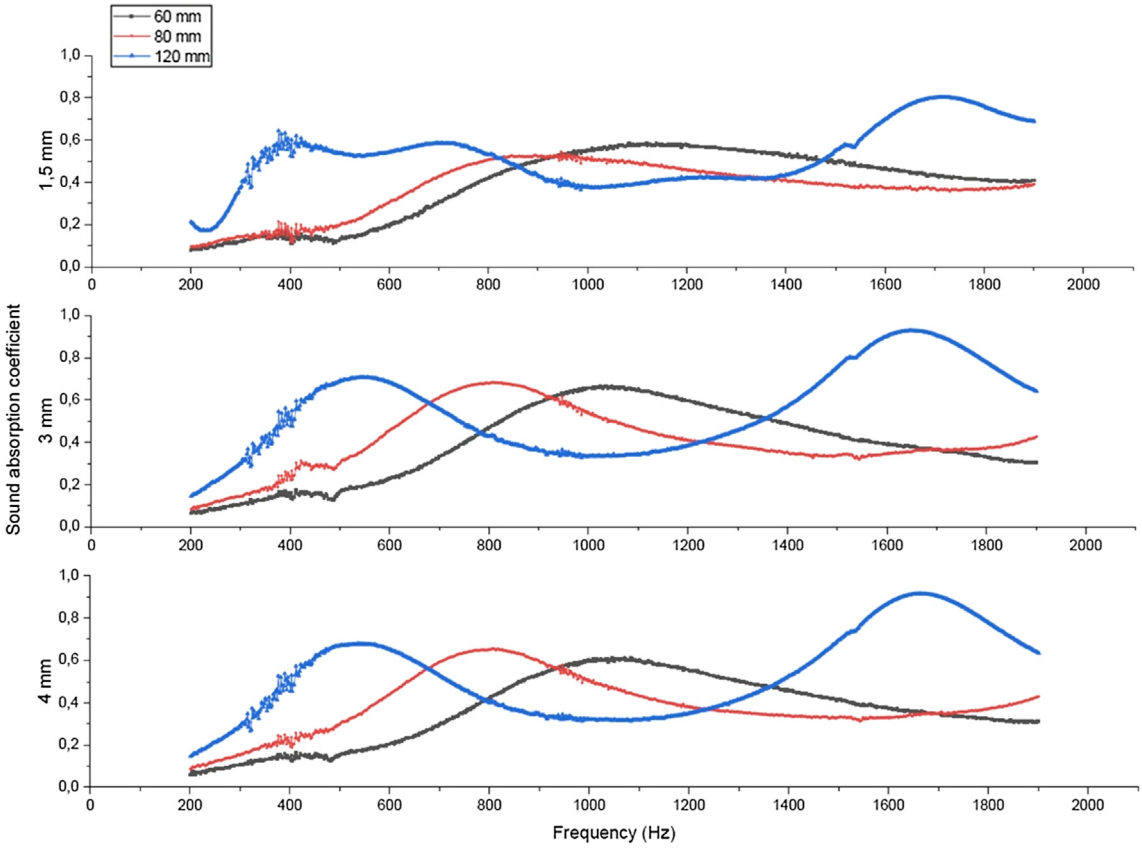

Fig. 6. Sound absorption coefficient values of 60 mm, 80 mm, and 120 mm thick samples and for 1.5 mm to 4 mm diameter broom fibers.

absorption for frequencies below 800 Hz for samples 60 mm thick and below 650 Hz for 80 mm thick samples.

3.2. Modelling the sound absorption coefficients using linear regression and artificial neural network

To appreciate the results obtained modelling the sound absorption coefficients, two algorithms were used. One based on neural networks, another based on multiple linear regression. Let's start with the model based on linear regression. Regression analysis was performed using generalized linear models (GLM).

In Table 2 are shown the RMSE, MAE and the Person's correlation coefficient for the multiple regression model.

The values in Table 2 will then be used to compare them with those obtained from the model based on neural networks.

Then a model based on artificial neural network was implemented. Fig. 7 shows the architecture of the model based on neural networks.

From the analysis of Fig. 7 it is possible to notice that five data inputs are presented to the network, respectively: thickness of the samples, diameter of the pieces of broom, resistivity, porosity, and frequency. Then a hidden layer with ten neurons is added. Finally, an output level with only one output is returned. The lines between neurons of different levels give an idea of the weight of the connection: the greater the thickness of the line, the greater the weight. While the colors of the lines indicate the sign of the connection: black means positive; gray means negative. In this way, it is possible to understand how the weights of the connections contribute to the output even in the case of layers with many neurons [50,51]. Tables 3 and 4 show the values of the best weights and biases obtained from the model.

Table 2
RMSE, MAE and the Person's correlation coefficient for the regression model.

RMSE	MAE	Person's Correlation Coefficient
0.147	0.130	0.571

In Table 5 are shown the RMSE, MAE and the Person's correlation coefficient for the artificial neural network model.

From the comparison between the two models, multiple regression and artificial neural network, we can obtain useful information on performance. From the comparison of the data reported in Tables 2 and 5, we can see that the model based on the artificial neural network shows better results: artificial neural network Person's correlation coefficient equal to 0.989 compared to 0.571 obtained with Generalized Linear Model. Furthermore, the artificial neural network model has a decidedly lower error with 0.026 compared to 0.147, with an order of magnitude less. The same goes for the MAE, 0.017 against 0.130, even in this case we have an order of magnitude less.

To appreciate the results obtained we can compare the trend of the acoustic absorption coefficient with the frequency between the measured values and those simulated with the model we have elaborated.

The trends of the simulated values are in good agreement with the absorption coefficient data measured with the impedance tube for normal incidence as reported in Fig. 8. Some small differences can be found at low frequencies, due to small irregularities due to the measurement: The very small sound absorption value (0.1–0.2) is influenced by the inter-reflections of the sound waves that affect the specimen during the acoustic measurements.

For specimens 60 mm thick, the curves of the simulated data fit almost perfectly on those of the measured values: At low frequencies they adapt better, due to the anomalies due to the uncertainties of the measurements already discussed previously. The same can be said for specimens 80 mm thick.

For specimens with a thickness of 120 mm and a diameter of 1.5 mm there are appreciable differences between the measured and simulated values in the frequency range between 500 Hz–70 0 Hz: The measured value of the absorption coefficient is more flattened due to the measurement conditions suboptimal probably resulting from a suboptimal position of the specimen during the measurement.

For specimens with a thickness of 120 mm and a diameter of fibers 3 and 4 mm at frequencies around 1800 Hz, at the second

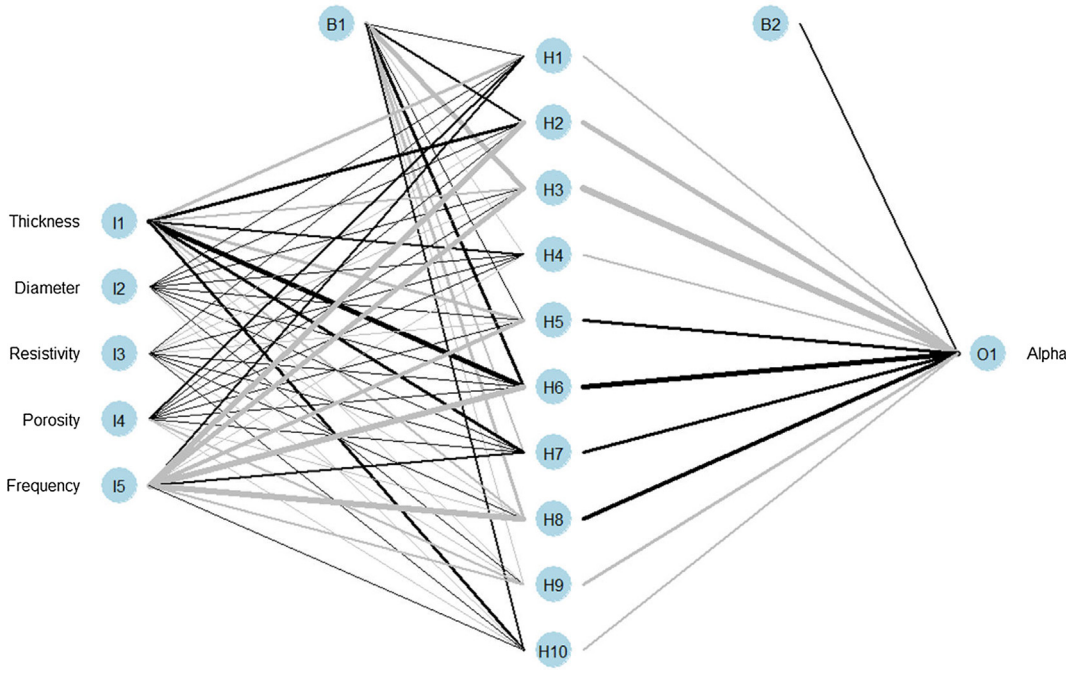

Fig. 7. Artificial neural network model architecture with three layers.

Table 3
Best weights and biases returned by the model (Input layer to Hidden layer).

	H1	H2	H3	H4	H5	H6	H7	H8	H9	H10
B1	0.675	1.3	−3.358	−0.018	0.704	1.756	−0.76	−1.498	−0.554	0.862
I1	−1.948	1.949	−1.029	1.169	−1.663	3.309	1.974	−1.453	−0.118	1.542
I2	0.181	0.258	0.324	0.098	0.257	0.236	0.142	−0.21	0.099	−0.196
I3	0.085	−0.026	−0.032	0.126	−0.102	0.011	0.001	0.004	−0.297	0.004
I4	0.751	0.556	0.703	0.688	0.29	0.628	0.357	−0.515	−0.793	−0.48
I5	1.156	−4.096	−3.518	−0.368	−2.637	−3.863	1.315	−4.287	−1.437	0.639

Table 4
Best weights and biases returned by the model (Hidden layer to Output layer).

B2–O1	H1–O1	H2–O1	H3–O1	H4–O1	H5–O1	H6–O1	H7–O1	H8–O1	H9–O1	H10–O1
0.859	−1.345	−3.618	−4.388	−1.302	2.024	3.001	1.952	2.887	−1.815	−1.204

Table 5
RMSE, MAE and the Person's correlation coefficient for the artificial neural network model.

RMSE	MAE	Person's Correlation Coefficient
0.026	0.017	0.989

maximum of the distribution, the measured value slightly overestimates the simulated value: This may be due to the upper limit of the measuring frequency imposed by the hypothesis of plane waves in the measuring tube and at the distance between the two microphones.

4. Conclusions

In this study, a new methodology was developed for the numerical modeling of the acoustic behavior of broom fibers. First, the characteristics of the different varieties of broom were examined and the procedures for processing the samples to be analyzed were described. Subsequently, the results of the measurements of the following acoustic properties of the material were analyzed: air flow resistance, porosity, and sound absorption coefficient. Finally, the results of the numerical modeling of the acoustic coefficient were reported using an algorithm based on artificial neural net-

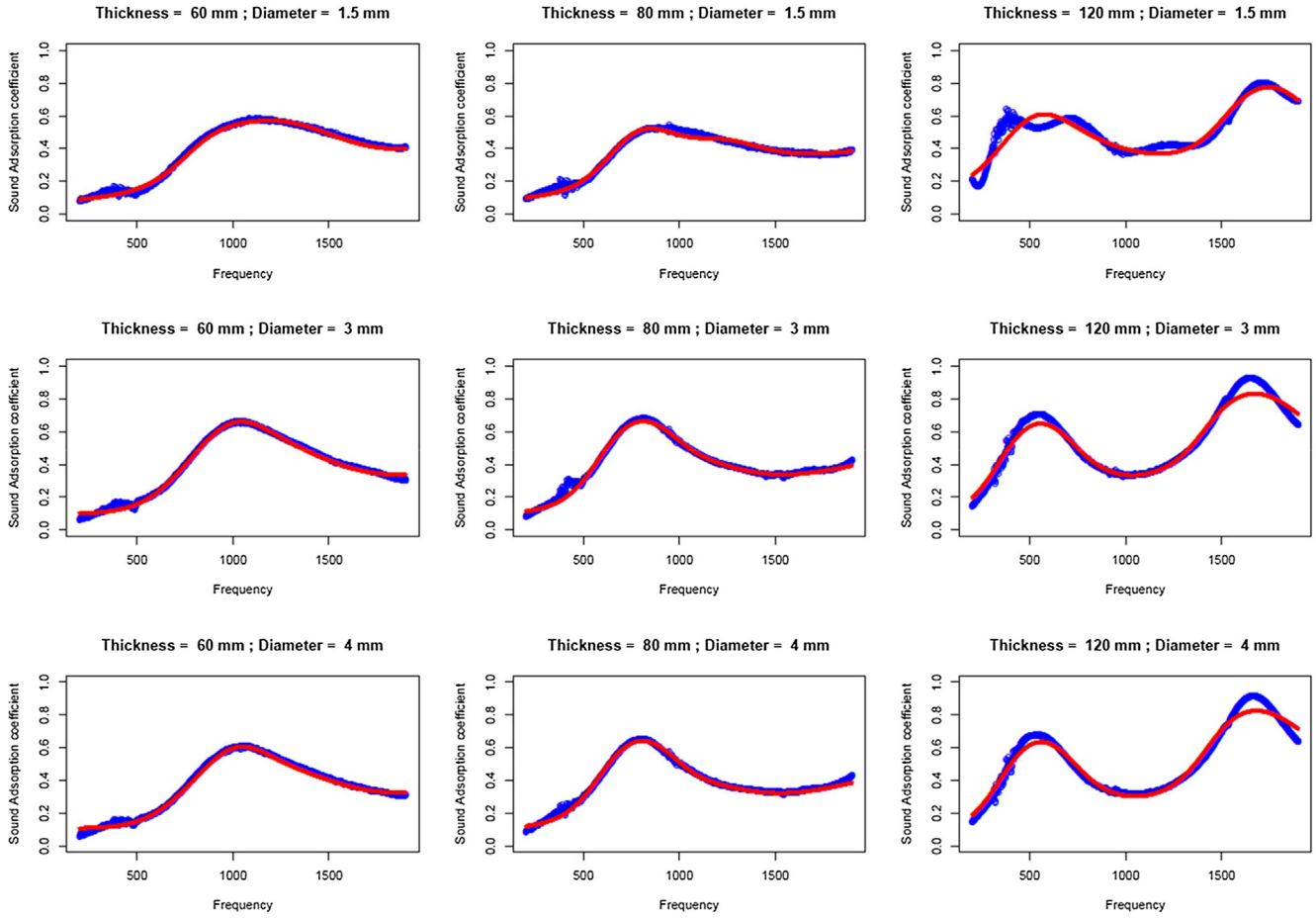

Fig. 8. Measured versus simulated trend of the acoustic absorption coefficient with frequency variation. The curve in blue represents the measured values, the curve in red those simulated. (For interpretation of the references to colour in this figure legend, the reader is referred to the web version of this article.)

works. The results obtained are compared with a model based on linear regression.

The model based on neural networks showed high values of the Pearson correlation coefficient (0.989), indicating a high number of correct predictions. A model for predicting the sound absorption coefficient can be extremely useful. Through the results of the model, it will be possible to evaluate the acoustic performance of a material for different configurations without the need to perform acoustic measurements.

Funding

This research received no external funding.

Declaration of Competing Interest

The authors declare that they have no known competing financial interests or personal relationships that could have appeared to influence the work reported in this paper.

Appendix A. Supplementary data

Supplementary data to this article can be found online at https://doi.org/10.1016/j.apacoust.2020.107239.

References

[1] Crocker J. Natural materials. Mater Technol 2008;23(3):174–8.
[2] Wegst UGK, Ashby MF. The mechanical efficiency of natural materials. Phil Mag 2004;84(21):2167–86.
[3] Wallenberger FT, Weston N, editors. Natural fibers, plastics and composites. Springer Science & Business Media; 2003.
[4] Ahmad F, Choi HS, Park MK. A review: natural fiber composites selection in view of mechanical, light weight, and economic properties. Macromol Mater Eng 2015;300(1):10–24.
[5] Chandramohan D, Marimuthu K. A review on natural fibers. Int J Res Rev Appl Sci 2011;8(2):194–206.
[6] Arenas JP, Crocker MJ. Recent trends in porous sound-absorbing materials. Sound Vibr 2010;44(7):12–8.
[7] Tg YG, Mr S, Siengchin S. Natural fibers as sustainable and renewable resource for development of eco-friendly composites: a comprehensive review. Front Mater 2019;6:226.
[8] Delany ME, Bazley EN. Acoustical characteristics of fibrous absorbent materials, In: Report of the National Physical Laboratory – Aerodynamics division; 1969.
[9] Miki Y. Acoustical properties of porous materials-modifications of Delany-Bazley models. J Acoust Soc Jpn (E) 1990;11(1):19–24.
[10] Allard JF, Champoux Y. New empirical equations for sound propagation in rigid frame fibrous materials. J Acoust Soc Am 1992;91(6):3346–53.
[11] Garai M, Pompoli F. A simple empirical model of polyester fibre materials for acoustical applications. Appl Acoust 2005;66(12):1383–98.
[12] Ramis J, Alba J, Del Rey R, Escuder E, Sanchís VJ. New absorbent material acoustic based on kenaf's fibre. Mater Constr 2010;60(299):133–43.
[13] Fatima S, Mohanty AR. Acoustical and fire-retardant properties of jute composite materials. Appl Acoust 2011;72(2–3):108–14.
[14] Oldham DJ, Egan CA, Cookson RD. Sustainable acoustic absorbers from the biomass. Appl Acoust 2011;72(6):350–63.
[15] Navacerrada MA, Díaz C, Fernández P. Characterization of a material based on short natural fique fibers. BioResources 2014;9(2):3480–96.
[16] Berardi U, Iannace G. Acoustic characterization of natural fibers for sound absorption applications. Build Environ 2015;94:840–52.
[17] Ginestar L, Del Deserto OIF. Spanish Broom (Spartium Junceum L.). In: Annual 2010/2011 of the Croatian Academy of Engineering, p. 23.
[18] Denton H. Ecological studies on seedlings of broom, Cytisus scoparius (L.) Link. Unpublished MSc thesis, London, UK: Imperial College; 1994.
[19] Blossey B, Notzold R. Evolution of increased competitive ability in invasive nonindigenous plants: a hypothesis. J Ecol 1995;83(5):887–9.
[20] Hosking JR. The feasibility of biological control of Cytisus scoparius (L) Link: report on overseas study tour, June–September 1990; 1990.
[21] ISO 9053, Acoustics – Materials for acoustical applications – Determination of airflow resistance; 2019.
[22] Garai M, Pompoli F. A European inter-laboratory test of airflow resistivity measurements. Acta Acust United Acust 2003;89(3):471–8.
[23] ISO 10534-1. Acoustics e Determination of Sound Absorption Coefficient and Impedance in Impedance Tubes – Part 1: Method Using Standing Wave Ratio; 1996.
[24] ISO 10534-2. Acoustics e Determination of Sound Absorption Coefficient and Impedance in Impedance Tubes – Part 2: Transfer-function Method; 1998.
[25] Iannace G, Ciaburro G, Trematerra A. Fault diagnosis for UAV blades using artificial neural network. Robotics 2019;8(3):59.
[26] Maxwell AE, Warner TA, Fang F. Implementation of machine-learning classification in remote sensing: an applied review. Int J Remote Sens 2018;39(9):2784–817.
[27] Iannace G, Ciaburro G, Trematerra A. Heating, ventilation, and air conditioning (HVAC) noise detection in open-plan offices using recursive partitioning. Buildings 2018;8(12):169.
[28] Butler KT, Davies DW, Cartwright H, Isayev O, Walsh A. Machine learning for molecular and materials science. Nature 2018;559(7715):547–55.
[29] Puyana Romero V, Maffei L, Brambilla G, Ciaburro G. Acoustic, visual and spatial indicators for the description of the soundscape of waterfront areas with and without road traffic flow. Int J Environ Res Public Health 2016;13(9):934.
[30] Beam AL, Kohane IS. Big data and machine learning in health care. JAMA 2018;319(13):1317–8.
[31] Romero VP, Maffei L, Brambilla G, Ciaburro G. Modelling the soundscape quality of urban waterfronts by artificial neural networks. Appl Acoust 2016;111:121–8.
[32] Rajkomar A, Dean J, Kohane I. Machine learning in medicine. N Engl J Med 2019;380(14):1347–58.
[33] Iannace G, Ciaburro G, Trematerra A. Wind turbine noise prediction using random forest regression. Machines 2019;7(4):69.
[34] Mahdavinejad MS, Rezvan M, Barekatain M, Adibi P, Barnaghi P, Sheth AP. Machine learning for Internet of Things data analysis: a survey. Digital Commun Networks 2018;4(3):161–75.
[35] Liakos KG, Busato P, Moshou D, Pearson S, Bochtis D. Machine learning in agriculture: a review. Sensors 2018;18(8):2674.
[36] Brunton SL, Noack BR, Koumoutsakos P. Machine learning for fluid mechanics. Annu Rev Fluid Mech 2019;52.
[37] Maffei L, Masullo M, Ciaburro G, Toma RA, Firat HB. Awaking the awareness of the movida noise on residents: measurements, experiments and modelling. In: Internoise 2019-Noise Control for a better environment. International Institute of Noise Control Engineering (I-Ince); 2019. pp. 1–10.
[38] Shanmuganathan S. Artificial neural network modelling: an introduction. In: Artificial Neural Network Modelling. Cham: Springer; 2016. p. 1–14.
[39] da Silva IN, Spatti DH, Flauzino RA, Liboni LHB, dos Reis Alves SF. Artificial neural network architectures and training processes. In: Artificial Neural Networks. Cham: Springer; 2017. p. 21–8.
[40] Vaidyanathan S, Volos C, editors. Advances and applications in chaotic systems. Berlin, Germany: Springer; 2016. Vol. 636, p. 445.
[41] Samarasinghe S. Neural networks for applied sciences and engineering: from fundamentals to complex pattern recognition. Auerbach Publications; 2016.
[42] Ciaburro G, Venkateswaran B. Neural Networks with R: smart models using CNN, RNN, deep learning, and artificial intelligence principles. Packt Publishing Ltd.; 2017.
[43] Riedmiller M, Braun H. A direct adaptive method for faster backpropagation learning: the RPROP algorithm. In: Proceedings of the IEEE International Conference on Neural Networks; March 1993. Vol. 1993, pp. 586–591.
[44] Møller MF. A scaled conjugate gradient algorithm for fast supervised learning. Neural Networks 1993;6(4):525–33.
[45] Ciaburro G. Regression Analysis with R: Design and develop statistical nodes to identify unique relationships within data at scale. Packt Publishing Ltd.; 2018.
[46] Darlington RB. Regression and Linear Models. New York, NY, USA: McGraw-Hill; 1990. p. 292–3 [Google Scholar].
[47] Hothorn T, Everitt BS. A handbook of Statistical Analyses Using R. Boca Raton, FL, USA: Chapman and Hall/CRC; 2014.
[48] Willmott CJ, Matsuura K. Advantages of the mean absolute error (MAE) over the root mean square error (RMSE) in assessing average model performance. Climate Res 2005;30(1):79–82.
[49] Dragonetti R, Iannace G, Ianniello C. Insertion loss of a heap of gravel outdoors. Acta Acust 2003;89:S56–7.
[50] Venables WN, Ripley BD. Modern Applied Statistics with S. fourth edition. Springer; 2002.
[51] Ripley BD. Pattern Recognition and Neural Networks. Cambridge; 1996.